Moroccan Journal of Chemistry
ISSN: 2351-812X
http://revues.imist.ma/?journal=morjchem&page=login
R. T. Loto / Mor. J. Chem. 5 N°1 (2017) 81-95

Evaluation of the synergistic properties of 4-hydroxy-3-methoxybenzaldehyde and 1, 4-diaminobenzene on the electrochemical corrosion behaviour of mild steel in dilute acid solutions

R.T. Loto(a,b)*, C.A Loto(a), A. Olaitan(b) and P. Babalola(a)

(a)Department of Mechanical Engineering, Covenant University, Ota, Ogun State, Nigeria
(b)Department of Chemical, Metallurgical & Materials Engineering, Tshwane University of Technology, Pretoria, South Africa

Abstract

The electrochemical corrosion behaviour of the synergistic effect of 4-hydroxy-3-methoxybenzaldehyde and 1, 4-diaminobenzene on mild steel in dilute sulphuric and hydrochloric acid solution (1M concentration) with 1.5% recrystallized sodium chloride evaluated with weight loss analysis, potentiodynamic polarization test and optical microscopy. Statistical analysis of the results was done with Two-way ANOVA to assess their statistical significance of the experimental variables on inhibition efficiency values. Results show the combined organic derivatives performed effectively in both acids with average inhibition efficiency values above 85%. Observations from optical microscopy images further confirm the results of experimental data. Statistical derivations reveal the overwhelming significance of exposure time only inhibition efficiency values in both acids.

* *Corresponding author:*
tolu.loto@gmail.com
Received 13 Nov 2016, Revised 05 Dec 2016, Accepted 02 April 2017

Keywords: *adsorption; corrosion, mild steel; inhibitor; hydrochloric; sulphuric*

1. Introduction

Metallic corrosion especially involving mild steel is a major industrial issue. Mild steel is an important structural material and is corroded by many agents, of which aqueous acids and chlorides are the most dangerous. The concealment of metallic alloys from corrosion causing ions is one of the most effective methods of inhibiting electrochemical corrosion. The use of corrosion inhibitors is usually one of the most suitable means to attain this purpose [1]. Recently, organic molecules of natural origin which displays strong affinity for metal surfaces are the target of research experimentation directed towards the evolution and advancement of biodegradable corrosion inhibitors. The corrosion prevention mechanism by which an inhibitor decreases corrosion rate is achieved through interference with some of the steps for the electrochemical process. Many studies have been carried out to find suitable compounds to be used as corrosion inhibitors for mild steel in different aqueous solutions. These studies reported that there are a number of organic and inorganic compounds which can inhibit corrosion of steel [2-4]. The effectiveness of organic inhibitors depends is the product of its degree of adsorption onto the metal surface, the adsorption depends mainly on the electronic structure of the organic moity. The planarity (p) and lone pairs of electrons present on atoms responsible for the inhibition reaction mechanism are important structural features that control the adsorption of these molecules onto the surface of the metal [5]. The research aims to investigate the corrosion inhibition properties of the combined mixture of 4-hydroxy-3-methoxybenzaldehyde and 1, 4-diaminobenzene on mild steel in 1M sulphuric and hydrochloric acid solution with sodium chloride addition through weight loss, potentiodynamic polarization and optical microscopy techniques.

2. Materials and Methods

2.1 Material

Mild steel was obtained commercially and its nominal composition was analyzed at the Advanced Materials and Tribo-corrosion Research Laboratory, Department of Chemical and Metallurgical Engineering, Tshwane University of Technology, Pretoria, South Africa. Its percentage nominal composition is shown in Table 1 below.

Table 1. Percentage nominal composition of mild steel

Carbon	Silicon	Manganese	Phosphorus	Sulphur	Copper	Aluminium	Iron
0.401	0.169	0.44	0.005	0.012	0.008	0.025	98.86

2.2 Inhibitor

An equal proportion of 4-hydroxy-3-methoxybenzaldehyde and 1, 4-diaminobenzene (HPD) in the combined form is the inhibitor used. Both compounds were obtained from Merck Chemical, Germany. The structural formula of 4-hydroxy-3-methoxybenzaldehyde is shown in Fig. 1a, and the molecular formula is $C_8H_8O_3$, while the structural formula of 1, 4-diaminobenzene is shown in Fig. 1b, and the molecular formula is $C_6H_4(NH_2)_2$, HPD was prepared in molar concentrations of 0.0048, 0.0096, 0.0144, 0.0192, 0.0240 and 0.0288, respectively.

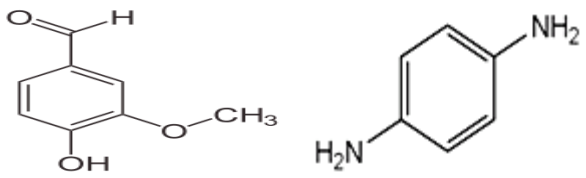

(a) (b)

Figure 1. Chemical structure of (a) 4-hydroxy-3-methoxybenzaldehyde, (b) 1, 4-diaminobenzene

2.3 Corrosive Test Media

200 ml of 1M of H_2SO_4 and 1M HCl acid were prepared from distilled water with added 1.5% recrystallized sodium chloride (analar grade) were used as the corrosion test media.

2.4 Preparation of Test Specimens

Cylindrical mild steel samples of 14 mm diameter were machined into specified number of test specimens, each with average dimensions of 10 mm in length. At the center of each sample was drilled a 3 mm hole for suspension and observation during the tests. Each test specimen was carefully cleansed with distilled water and acetone for weight loss analysis. Preparation of the test specimens for potentiodynamic polarization test involve mounting in resin material and after curing their exposed surface ends are grinded with silicon carbide abrasive papers of 80, 120, 220,800 and 1000 grits.

2.5 Weight-loss Analysis

Weighed steel specimens were each immersed in 200ml of the acid test solution at specific concentrations of the HPD for 504 h at ambient temperature. The steel specimens were taken out every 72 h and weighed after cleansing with distilled water and acetone. Plots of corrosion rate (mm/y) (calculated) versus exposure time (h) (Figs. 2 & 7) for the two acid media and those of percentage inhibition efficiency (%*IE*) (calculated) versus exposure time (h) (Fig. 8 & 9) were produced from data tabulated Tables 1 & 2

Where θ is the quantitative amount of inhibitor adsorbed per gram (or kg) of the steel specimen. M_1 and M_2 are the weight loss of mild steel in the inhibited and uninhibited acid test solutions.

2.6 Potentiodynamic Polarization Analysis

Potentiodynamic polarization test was done on cylindrical mild steel specimens embedded in resin plastic mounts with exposed surface area of 154 mm^2 at ambient temperature of 25 ^oC with Digi-Ivy potentiostat. A platinum rod was used as the counter electrode and silver chloride electrode (Ag/AgCl) with pH of 6.5 was used as the reference electrode. The potentials was scanned from -1.5V to +1.5 V at a scan rate of 0.002V/s. Corrosion current (i_{corr}), corrosion current density (I_{corr}) and corrosion potential (E_{corr}) were calculated from the Tafel plots of potential versus log I_{corr}.

2.7 Optical Microscopy Characterization

The surface morphology and topography of the inhibited and uninhibited steel samples was studied after weight-loss analysis in 1 M H_2SO4 and 1 M HCl solutions using Omax trinocular metallurgical microscope micrographs were recorded.

2.8 Statistical Analysis

Two-factor single level statistical analysis with ANOVA software (*F*-test) was used to determine the statistical relevance of specific HPD concentrations and exposure time on the inhibition efficiency values of HPD in H_2SO_4 and HCl acid solutions. The *F*-test was used to study the quantitative value of variation within each of the samples relative to the amount of variation between the samples.

3. Theory and Calculation

The corrosion rate (*R*) from weight loss test was calculated from equation 1 below:

$$R = \left[\frac{87.6M}{DAT}\right] \quad (1)$$

M is the weight loss in milligrams, D is the density in g/cm^2, A is the area in cm^2, and T is the time of exposure in hours. The %IE was determined from equation 2.

$$\%IE = \left[\frac{R_1 - R_2}{R_1}\right] * 100 \quad (2)$$

R_1 and R_2 are the corrosion rates in the presence and absence of specific concentrations of HPD. The %IE was determined after 72 h consecutively through the research. The surface coverage is determined from equation 3:

$$\theta = \left[1 - \frac{M_2}{M_1}\right] \quad (3)$$

The corrosion rate (R) for potentiodynamic polarization analysis was calculated from equation 4 below;

$$R = \frac{0.00327 * i_{corr} * E_q}{D} \quad (4)$$

i_{corr} is the current density in µA/cm^2, D is the density in g/cm^3; E_q is the specimen equivalent weight in grams. The percentage inhibition efficiency (%IE) was determined from equation 5.

$$\%IE = 1 - \left[\frac{c2}{c1}\right] * 100 \quad (5)$$

$R_1$and R_2 are the corrosion current densities with and without HPD respectively.

The results for statistical analysis are calculated as follows;

The Sum of squares among columns (exposure time) was obtained with equation 6.

$$SS_c = \frac{\sum T_c^2}{nr} - \frac{T^2}{N} \quad (6)$$

Sum of Squares among rows (VAL concentration) was obtained with equation 7.

$$SS_r = \frac{\sum T_r^2}{nc} - \frac{T^2}{N} \quad (7)$$

While the Total Sum of Squares was obtained from equation 8.

$$SS_{Total} = \sum x^2 - \frac{T^2}{N} \quad (8)$$

4. Results and discussion

4.1 Weight-loss analysis

The results for weight-loss (M), corrosion rate (R) and percentage inhibition efficiency (%IE) for the inhibiting compound on mild steel in the acid test solutions are presented in Tables 2 & 3. Fig. 2(a,b) & 3(a,b) shows the graphical illustration of corrosion rate and percentage inhibition efficiency against the time of exposure in 1M H_2SO_4 and 1M HCl acid. The synergistic effect of the combined mixture of 4-hydroxy-3-methoxybenzaldehyde and 1, 4-diaminobenzene (HPD) on the inhibited and uninhibited mild steel specimens is clearly distinct as displayed in the figures earlier mentioned due to its electrochemical influence on the reduction-oxidation corrosion reactions. Fig. 2(a) illustrates a sharp reduction in corrosion rate for 0.125% HPD to 0.75% HPD in contrast 0% HPD. The decrease in corrosion rate occurs from the onset of the exposure hours to 504h. During this period the corrosion rate remained generally constant through. This phenomenon is similar to what is obtained in Fig. 3(a). This behaviour could be attributed to the increase of the surface coverage (θ) by the adsorption of the inhibitor on the steel surface. It shows that the electrochemical behaviour and inhibition mechanism of HPD in H_2SO_4 and HCl are similar. The ability of the molecule to chemisorb on the steel surface depends on the heteroatoms within its molecular structure and the electron density on these atoms [6]. The molecules present block the surface of mild steel via adsorption mechanism onto the metal surface reducing the available area for the attack of aggressive ions such as SO_4^{2-}or Cl^-. Fig. 2(b) and 3(b) shows the plot of inhibition efficiency against inhibitor concentration. Their observation shows that increase in

inhibitor concentration does not produce any significant change in inhibition efficiency. The inhibition efficiency of HPD as shown in the figures earlier mentioned is indirectly proportional to its concentration and corrosion rate.

Table 1. Data obtained from weight loss measurements for mild steel in 1 M H_2SO_4 at specific concentrations of HPD after 504 h

Specimens	Corrosion Rate (mmpy)	Surface Coverage (θ)	Weight Loss (mg)	Inhibition Efficiency (%)	Inhibitor Concentration (%)	Inhibitor Concentration (Molarity)
A	11.93	0	4.0355	0	0	0
B	1.05	0.912	0.3551	91.2	0.125	0.0048
C	1.20	0.899	0.4073	89.9	0.25	0.0096
D	1.36	0.886	0.4611	88.6	0.375	0.0144
E	0.99	0.917	0.3357	91.7	0.5	0.0192
F	0.41	0.966	0.1374	96.6	0.625	0.0240
G	1.42	0.881	0.4813	88.1	0.75	0.0288

Table 1. Data obtained from weight loss measurements for mild steel in 1 M HCl at specific concentrations of HPD after 504 h

Specimens	Corrosion Rate (mmpy)	Surface Coverage (θ)	Weight Loss (mg)	Inhibition Efficiency (%)	Inhibitor Concentration (%)	Inhibitor Concentration (Molarity)
A	13.8968	0	2.9583	0	0	0
B	2.11108	0.848	0.4494	84.8	0.125	0.004802
C	1.54784	0.889	0.3295	88.9	0.25	0.009605
D	1.55019	0.888	0.33	88.9	0.375	0.014407
E	1.47174	0.894	0.3133	89.5	0.5	0.019209
F	1.41584	0.898	0.3014	89.8	0.625	0.024012
G	1.43322	0.897	0.3051	89.7	0.75	0.028814

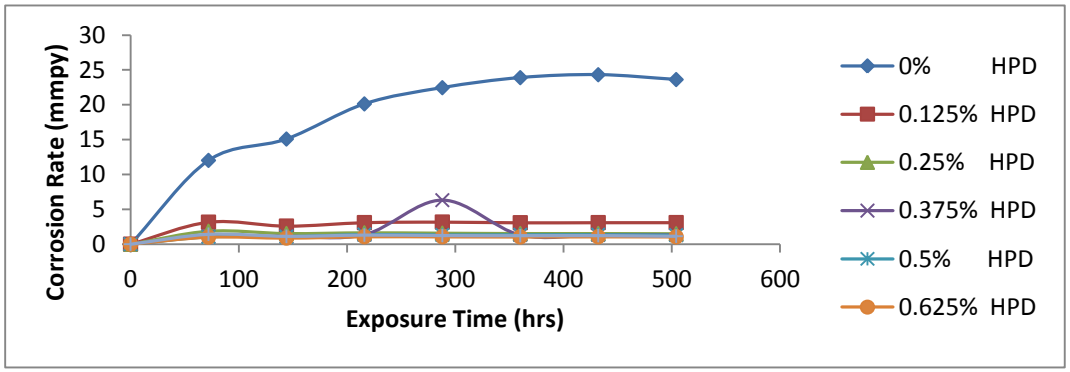

(a)

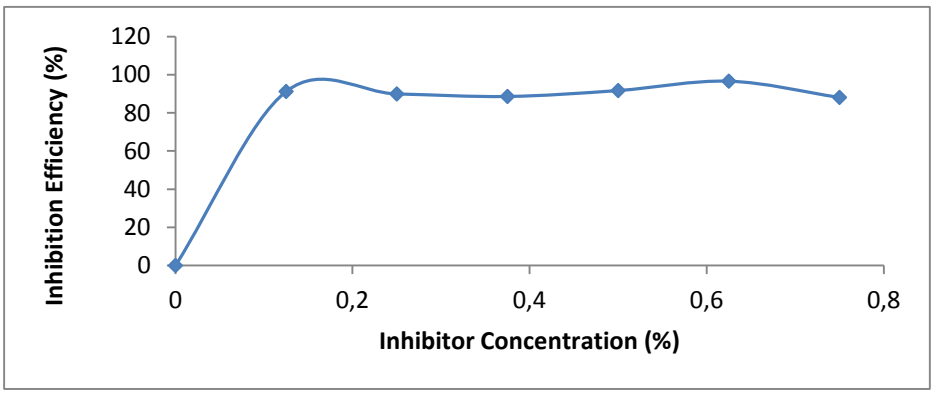

(b)

Figure 2. Plot of (a) corrosion rate against exposure time (b) inhibition efficiency against inhibitor concentration in 1 M H_2SO_4 at 0%-0.75% HPD

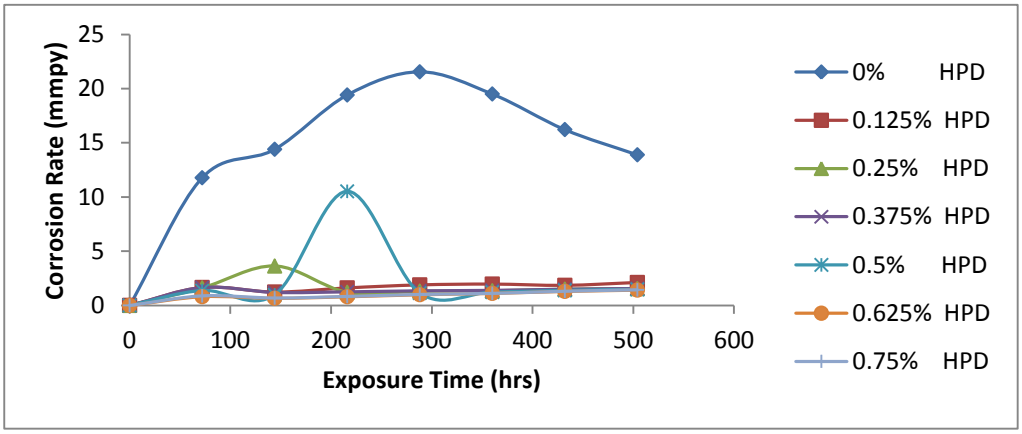

(a)

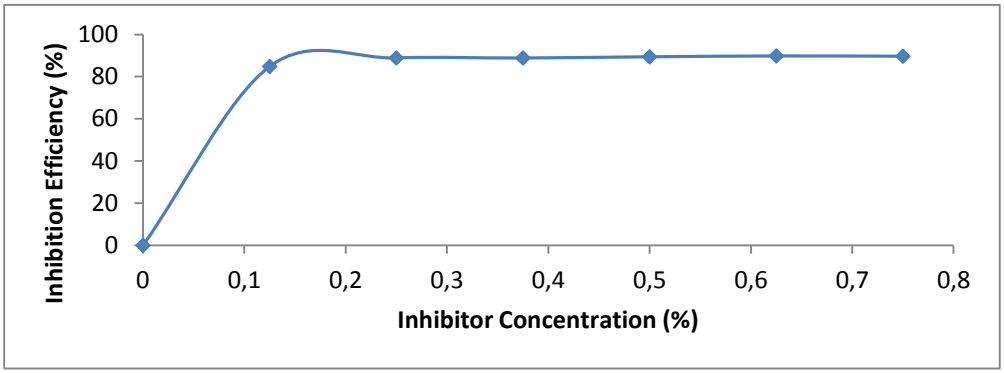

(b)

Figure 3. Plot of (a) corrosion rate against exposure time (b) inhibition efficiency against inhibitor concentration in 1 M HCl at 0%-0.75% HPD

4.2 Polarization studies

The electrochemical influence of HPD on the corrosion polarization behaviour of mild steel in 1 M H_2SO_4 and HCl solutions is shown in Fig. 4 to Fig. 7. Fig. 4 shows the potentiodynamic polarization diagram of the log of current

density *I* ($mAcm^{-2}$) against corrosion potential *E* (mV) for mild steel for in 1 M H_2SO_4, while Fig. 5 shows the diagram of %*IE* against HPD compound at specific concentrations in the acid solution. Results of the potentiodynamic test are shown in Table 4. Observation of the table shows a slight progressive increase in inhibition efficiency of HPD with increase in its concentration from 0.0048M to 0.0240M at which the inhibition efficiency is optimal (96.55%), after which the was a slight decrease at 0.0288M to 94.04%. The result shows that HPD effectively inhibited the mild steel specimens at all concentrations studied in H_2SO_4 acid. The progressive increase in inhibition efficiency is significant as higher inhibition efficiency causes a proportionate decrease in corrosion rate and hence increases corrosion resistance.

The graphical illustration of log of current density I (Acm^2) against corrosion potential *E* (mV) for HPD in 1 M HCl is shown in Fig.6. Fig. 7 shows the graphical illustration of %*IE* against HPD concentrations from the potentiodynamic polarization test. Test results from the polarization test are shown in Table 5 wherewith HPD exhibited similar electrochemical behaviour in HCl acid as compared to H_2SO_4. There was a marginal but progressive increase in inhibition efficiency as HPD concentration increases with the highest inhibition efficiency of 91.29% at 0.0288M. The corrosion rate values in HCl are generally similar to the values in H_2SO_4 due to the more aggressive nature of SO_4^{2-} ions in H_2SO_4 solution. VAL exhibited similar potency in HCl as in H_2SO_4 in inhibiting corrosion of the mild steel samples under study

Analysis of the polarization plots in Fig. 4 and Fig. 5 shows anodic and cathodic inhibition properties as the plots alternates between anodic and cathodic potentials. This is corroborated from the corrosion potential values shown in Tables 4 and 5. The corrosion potentials shift between higher and lower potentials as HPD concentration increases coupled with a significant decrease in corrosion rate due to adsorption over the metal surface. This is as a result of the stifled redox corrosion reaction involving hydrogen evolution, oxygen reduction and anodic dissolution. The inhibition mechanism in H_2SO_4 and HCl is the mixed type because the maximum change in corrosion potential is 36mV in H_2SO_4 and 16mV in HCl however they show strong tendency for cathodic inhibition [7, 8].

Previous research on the corrosion inhibition behaviour of 1, 4-diaminobenzene on mild steel in H_2SO_4 shows that the compound exhibited inhibition efficiency values that progressively increased from values below 10% at lowest concentration to a value above 70% before decreasing sharply to values below 10% at maximum concentration [9]. This effect is as a result of desorption of the inhibitor molecules from the steel surface due to lateral repulsion between the inhibitor molecules [10, 11]. A different phenomenon was observed for mild steel in HCL where the inhibition efficiency values were generally below 40% with the exception of one particular concentration where the inhibition efficiency was above 90%. The results show that the inhibition performance of 1, 4-diaminobenzene is strongly subject to/dependent on its concentration. Study of the effect of 1, 4-diaminobenzene on austenitic stainless steel (type 304) in dilute HCl concentrations shows similar phenomenon to the effect of 1, 4-diaminobenzene on mild steel in H_2SO_4 [12].

Unpublished report on the corrosion inhibition effect of 4-hydroxy-3-methoxybenzaldehyde on mild steel in H_2SO_4 and HCl acid shows that the compound performed excellently at all concentrations studied however, the inhibition efficiency but there is no direct relationship between the inhibitor concentration and inhibition efficiency. Changes in inhibitor concentration did not produce any remarkable change in inhibition efficiency. The synergistic effect of 4-hydroxy-3-methoxybenzaldehyde and 1, 4-diaminobenzene results in corrosion inhibition performance that differs slightly. The inhibition efficiency value is above 85% in H_2SO_4 and HCl at lowest concentration and the values increased progressively. Increase in inhibitor concentration results in increase inhibition efficiency. Observation of data from previous and current research shows the inhibition efficiency is of the mixed type with the exception of mild steel in HCl where the inhibitor is overwhelmingly cathodic

Table 4. Potentiodynamic polarization test data for mild steel in 1 M H_2SO_4 at specific HPD concentrations.

Specimen	Inhibitor Conc. (Molarity)	Corr. Rate (mmpy)	Inhibition Efficiency (%)	Corr. Current (A)	Corr. Current Density (A/cm^2)	Corr. Potential (V)	Polarization resistance, R_p	B_c	B_a
A	0	8.73	0	1.16E-03	7.51E-04	-0.273	-240.68	-0.856	31.700
B	0.0048	1.02	88.32	1.35E-04	8.77E-05	-0.306	-717.80	-0.806	1.308
C	0.0096	0.99	88.68	1.31E-04	8.49E-05	-0.289	-592.94	-0.691	1.429
D	0.0144	0.71	91.83	9.44E-05	6.13E-05	-0.300	-740.42	-0.681	1.510
E	0.0192	0.48	94.52	6.33E-05	4.11E-05	-0.289	-638.12	-0.685	1.970
F	0.0240	0.30	96.55	3.99E-05	2.59E-05	-0.301	-616.21	-0.723	1.620
G	0.0288	0.52	94.04	6.89E-05	4.47E-05	-0.309	-827.90	-0.732	1.200

Table 5. Potentiodynamic polarization test data for mild steel in 1 M HCl at specific VAL concentrations.

Specimen	Inhibitor Conc. (Molarity)	Corr. Rate (mmpy)	Inhibition Efficiency (%)	Corr. Current (A)	Corr. Current Density (A/cm^2)	Corr. Potential (V)	Polarization resistance, R_p	B_c	B_a
A	0	12.23	0	1.62E-03	1.05E-03	-0.316	-431.35	-0.677	1.186
B	0.0048	1.73	85.82	2.30E-04	1.49E-04	-0.326	-271.23	-0.755	16.050
C	0.0096	1.47	88.02	1.94E-04	1.26E-04	-0.312	-333.83	-0.712	13.140
D	0.0144	1.45	88.17	1.92E-04	1.24E-04	-0.320	-425.47	-0.672	11.910
E	0.0192	1.25	89.76	1.66E-04	1.08E-04	-0.322	-450.03	-0.715	19.974
F	0.0240	1.37	88.83	1.81E-04	1.17E-04	-0.322	-341.54	-0.696	17.770
G	0.0288	1.06	91.29	1.41E-04	9.16E-05	-0.332	-350.05	-0.750	13.785

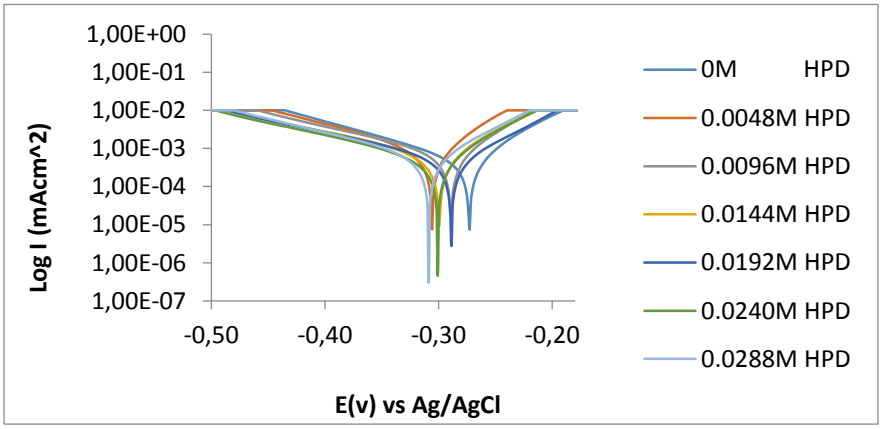

Figure 4. Potentiodynamic polarization plot for mild steel in 1 M H_2SO_4 acid at specific HPD concentrations (0.008M – 0.049M)

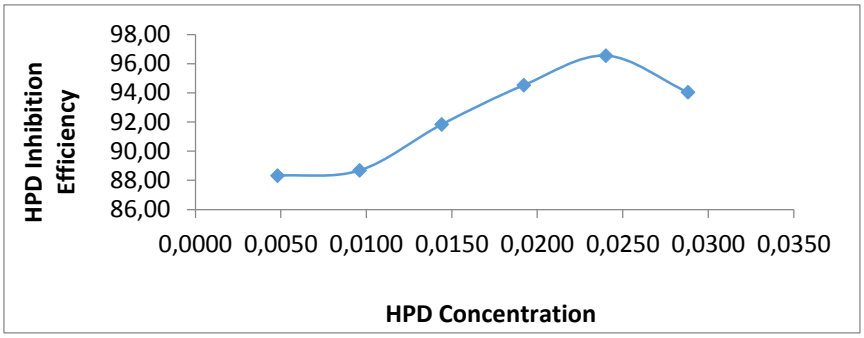

Figure 5. Plot of %*IE* versus HPD inhibitor concentration for potentiodynamic polarization test in 1 M H_2SO_4

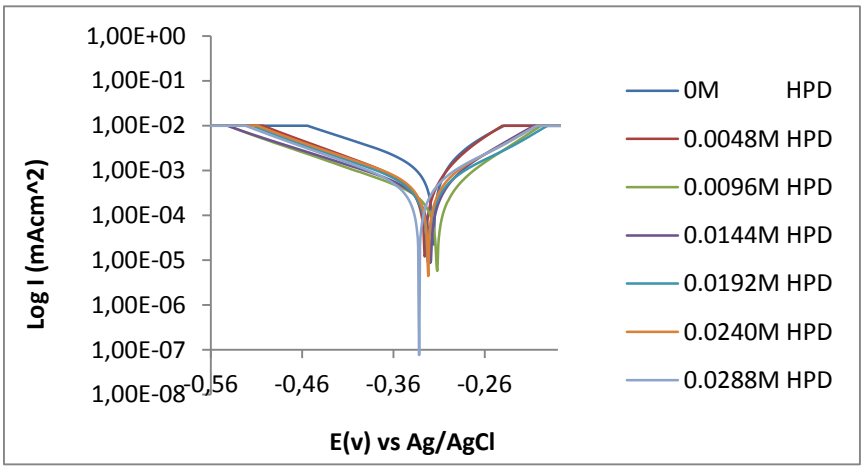

Figure 6. Potentiodynamic polarization plot for mild steel in 1 M HCl acid at specific VAL concentrations (0.008M – 0.049M)

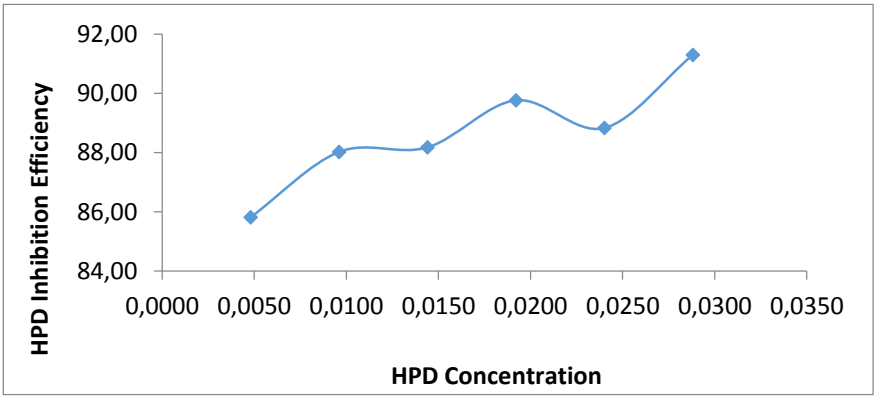

Figure 7. Plot of %*IE* versus VAL inhibitor concentration for potentiodynamic polarization test in 1 M HCl

4.3 Adsorption isotherm

The mechanism of corrosion inhibition can be explained on the basis of the adsorption behaviour of the adsorbate on the metal surface through the use of adsorption isotherms [13]. Adsorption isotherm is an exceptional plot which relates the phenomenon controlling the retention, discharge or movement of adsobate from the aqueous solution to the solid-interphase at a constant temperature [14, 15]. The physicochemical parameters of HPD together with the thermodynamic assumptions that governs the organo-metallic relationship in the corrosive medium, provides sufficient insight into the mechanism of adsorption, surface and topographical characteristics and the extent of adsorption of HPD to the metal surface [16]. Langmuir adsorption isotherms produced the best fit the experimental

results. The Langmuir equation assumes that the adsorption reaction involves a single reaction with a constant energy of adsorption [17]. Langmuir isotherm points to homogeneous adsorption over the metal surface, wherewith the inhibitor molecule has constant enthalpies and sorption activation energy [18]. The conventional form of the Langmuir isotherm is,

$$\left[\frac{\theta}{1-\theta}\right] = K_{ads}C \quad (9)$$

and rearranging gives

$$\left[\frac{c}{\theta} = \frac{1}{\theta}\right] + C \quad (10)$$

where θ is the value of surface coverage on the steel alloy, C is VAL concentration in the acid solution, and K_{ads} is the equilibrium constant of the adsorption process (representing the degree of adsorption, higher values of K_{ads} indicates that the inhibitor is strongly adsorbed on the metal surface). The plots of $\frac{C}{\theta}$ versus the inhibitor concentration C were linear (Fig. 8 and 9) indicating Langmuir adsorption. The following assumption is valid with the Langmuir isotherm model

- The alloy surface contains the adsorption sites which are assumed to be perfectly flat plane for a homogeneous surface.
- The adsorbing molecule adsorbs into an immobile state.
- All sites are equivalent.
- Each site holds a maximum of one molecule i.e. mono-layer coverage only.
- There are no interactions between adsorbate molecules on adjacent sites on the alloy surface [19].

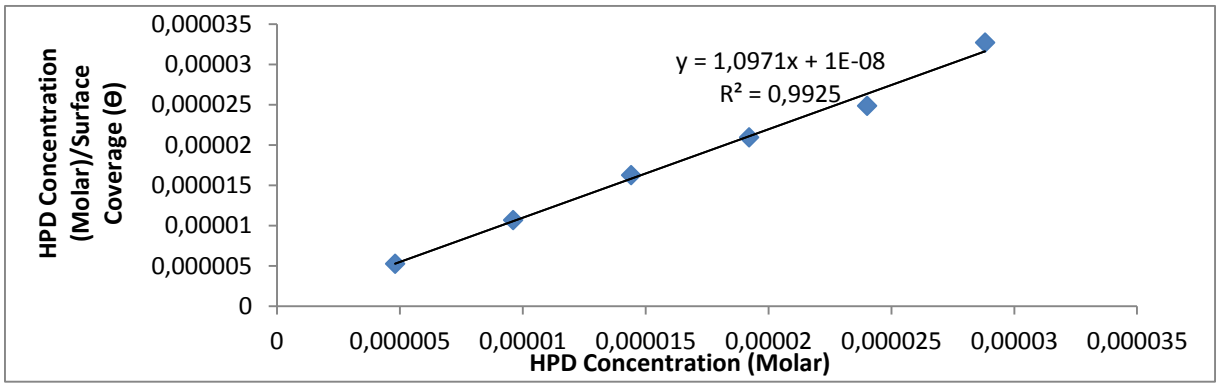

Figure 8. Graph of $\frac{C}{\theta}$ against HPD concentration (C) in 1 M H_2SO_4

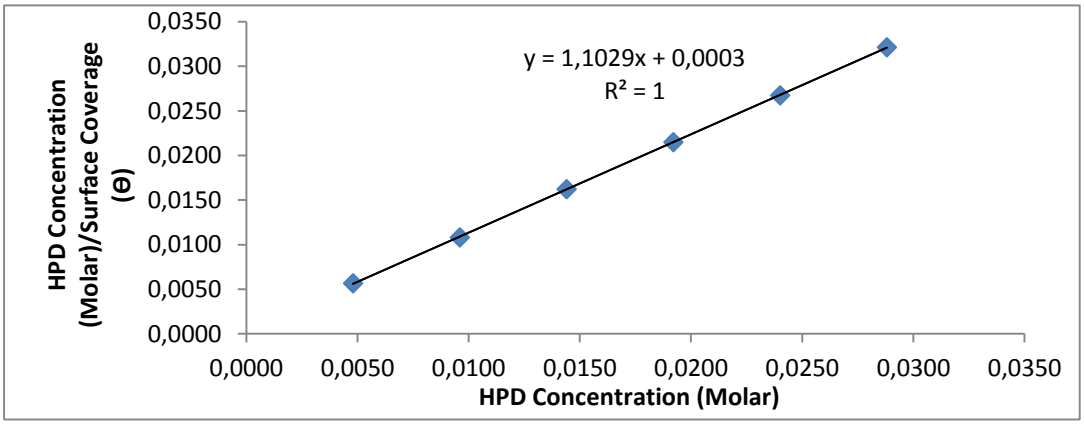

Figure 9. Graph of $\frac{C}{\theta}$ versus HPD concentration (C) in 1 M HCl

However due to competitive adsorption between HPD molecules and the corrosive ions (SO_4^{2-} and Cl^-) compete for the same adsorption sites, the following assumptions are application during the metal inhibitor interaction.

- Each site can hold at most one molecule of HPD or one molecule of (SO_4^{2-} and Cl^-), but not both.
- There are no interactions between adsorbate molecules on adjacent sites [20].

The line in Fig. 8 & 9 had a slope of 1.0971 and 1.1029, while the correlation coefficient (R^2) is 0.9925 and 1. The slight deviation of the slope from unity shows that the HPD molecules occupy specific typical adsorption site at the metal/solution interface and it assumes monolayer adsorption (i.e. the adsorbed layer is one molecule in thickness) [21-24].

4.4 Thermodynamics of the corrosion process

The values of Gibbs free energy (ΔG_{ads}) and the equilibrium adsorption constant (K_{ads}) were obtained for the Langmuir isotherms using equation (11) and listed in Tables 5 & 6.

$$\Delta G_{ads} = -2.303RT \log [55.5K_{ads}] \quad (11)$$

Where 55.5 is the molar concentration of water in the solution, R is the universal gas constant, T is the absolute temperature. K_{ads} is related to surface coverage (θ) by the following equation.

$$K_{ads}C = \left[\frac{\theta}{1-\theta}\right] \quad (12)$$

Table 5. Values obtained for Gibbs free energy, surface coverage and equilibrium constant of adsorption at specific concentrations of HPD in 1 M H_2SO_4

Samples	Surface Coverage (θ)	Molarity ($M*10^3$)	Equilibrium Constant of Adsorption (K)	Gibbs Free Energy, (ΔG) (KJ/mol)
A	0	0	0	0
B	0.912	4.80E-06	2158041	-36.13
C	0.899	9.60E-06	926735	-34.03
D	0.886	1.44E-05	539455	-32.69
E	0.917	1.92E-05	575147	-32.85
F	0.966	2.40E-05	1183248	-34.64
G	0.881	2.88E-05	256936	-30.85

Table 6. Values obtained for Gibbs free energy, surface coverage and equilibrium constant of adsorption at specific concentrations of HPD in 1 M HCl

Specimen	Surface Coverage (θ)	Molarity ($M*10^3$)	Equilibrium Constant of Adsorption (K)	Gibbs Free Energy,(ΔG) (KJ/mol)
A	0		0	0
B	0.848	4.8E-06	1162513	-38.00
C	0.889	9.6E-06	830653	-37.66
D	0.888	1.4E-05	552824	-40.94
E	0.894	1.9E-05	439494	-38.06
F	0.898	2.4E-05	367121	-37.43
G	0.897	2.9E-05	301803	-37.66

Generally, the values of ΔG_{ads} up to -20 KJ/mol are constant with the electrostatic interaction (physisorption) between the ionized molecules of HPD and charged metal surface, while negative values around -40 KJ/mol involve sharing or charge transfer of electrons from HPD compound to the metal surface to form a coordinate type of bond (Chemisorption) [25]. The obtained values of ΔG_{ads} ranges between -36.13 kJ mol^{-1} and -30.85 kJ mol^{-1} in H_2SO_4 solutions while in HCl it varies between -38.0 KJ mol^{-1} and -37.66 KJ mol^{-1} indicating physiochemical to chemical interaction in H_2SO_4 and chemisorption adsorption mechanism in HCl. The negative values of ΔG_{ads} indicate that these inhibitors are strongly adsorbed onto the mild steel surface.

4.5 Optical Microscopy

The micrographs from optical microscopy observation are shown from Fig. 10a to 13b. Fig. 10a & 10b shows the microscopy image of the steel samples before immersion into the acid solution. The uneven surface is due to machining of the sample before weight loss test. It presents the sample as received. Fig. 11a & 11b shows the optical microscopy observation of the control (without HPD inhibitor) samples after exposure hours from the acid media. Surface deterioration is clearly visible due to the action of cl- and SO42- ions in interaction with the metal cations that results in the anodic dissolution of the metal surface. The image clearly contrasts the image in Fig. 10. Figure 11b shows the presence of intergranular voids due to severe corrosion at the grain boundaries. Fig. 12a & b shows the microscopy image of the steel samples from H_2SO_4 acid solution with HPD inhibitor after exposure hours, while Figure 13a & b shows the microscopy image of the steel samples from HCl acid solution with HPD inhibitor after exposure hours. As earlier mention in the from the discussion from the potentiodynamic polarization section, HPD inhibits corrosion of the mild steel through adsorption onto the steel surface. This is clearly evident from observation of the micrograph in Fig. 12 and 13. The remants of the inhibitor is still visible giving the sample surface as it forms a protective film over the steel which acts as a potent barrier against the corrosive anions.

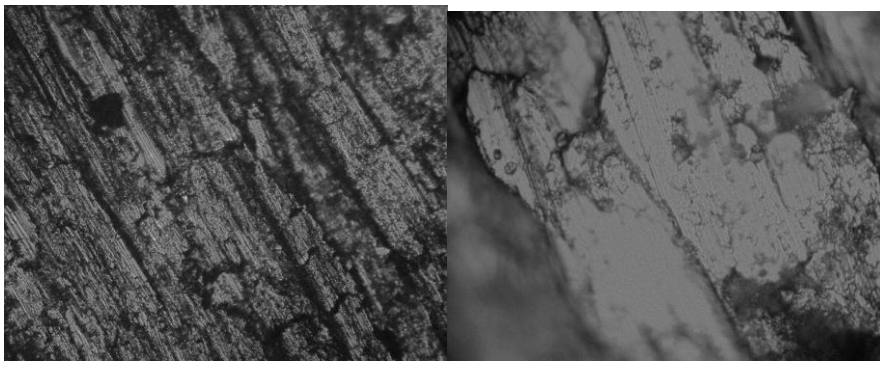

(a) (b)

Figure 10. Optical micrograph images of mild steel before corrosion (a) mag.x40, (b) mag.x100

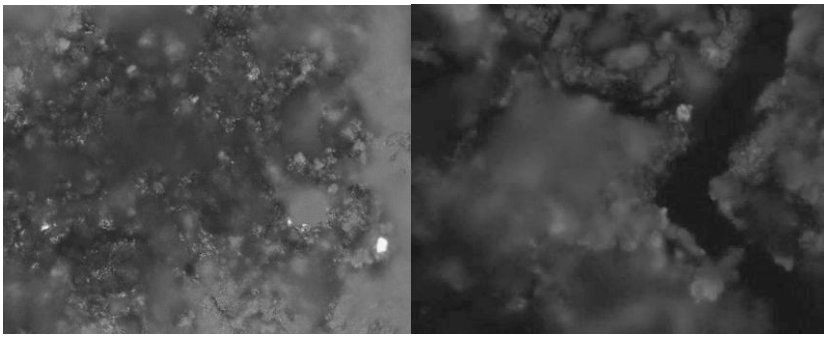

(a) (b)

Figure 11. Optical micrograph images of mild steel after corrosion without HPD inhibitor (a) mag.x40, (b) mag.x100

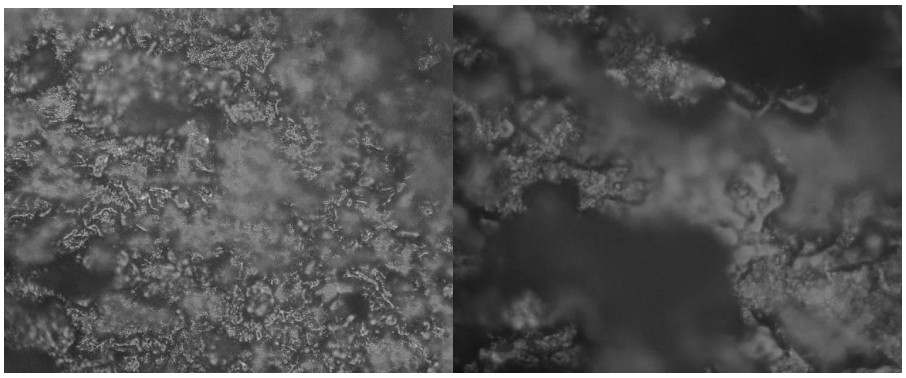

(a) (b)

Figure 12. Optical micrograph images of mild steel after corrosion with HPD inhibitor from H_2SO_4 solution (a) mag.x40, (b) mag.x100

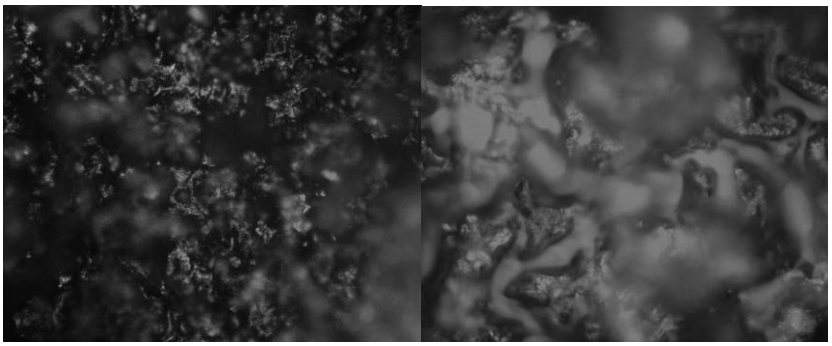

Figure 13. Optical micrograph images of mild steel after corrosion with HPD inhibitor from HCl solution (a) mag.x40, (b) mag.x100

4.6 Statistical Analysis

Two-way ANOVA was used to determine the effect of exposure time and HPD concentration on HPD inhibition efficiency values. The experimental HPD inhibition efficiency results in uninhibited and inhibited 1 M H_2SO_4 and HCl acids as a function of exposure time and HPD inhibitor concentrations are given in Tables 7 and 8. This technique based on variance ratios to determine if significant differences exist among the means of several groups of observation. The results clearly show that exposure time at 95% confidence level respectively have a significant effect on HPD inhibition efficiency in both acids. Data from ANOVA showed that the exposure time in both acid test solutions is statistically significant on the inhibition efficiency with F-values of 8.64 and 7.68 which is greater than the significance factor in the Tables (Tables 7 & 8) at $\alpha = 0.05$, thus they are significant at that level of probability. The statistical significance of exposure time on HPD is 253.1% and 209.3% in H2SO4 and HCl respectively depicting the overwhelming influence exposure time on the values of inhibition efficiency from the experiments in comparison to the HPD concentration which is negligible.

Table 7. Analysis of variance (ANOVA) for inhibition efficiency of HPD inhibitor in 1 M H_2SO_4 (at 95% confidence level)

Source of Variation	Source of Variation	Sum of Squares	Degree of Freedom	Mean Square	Mean Square Ratio (F)	Min. MSR at 95% confidence Significance F	F (%)
Among Columns	Inhibitor concentration	58850.57	5	11770.11	-12.27	2.53	-299.6
Among Rows	Exposure Time	-49718.2	6	-8286.37	8.64	2.42	253.1
Residual	Residual	-28778.9	30	-959.3			
Total	Total	-19646.5	41				

Table 8. Analysis of variance (ANOVA) for inhibition efficiency of HPD inhibitor in 1 M HCl (at 95% confidence level)

Source of Variation	Source of Variation	Sum of Squares	Degree of Freedom	Mean Square	Mean Square Ratio (F)	Min. MSR at 95% confidence Significance F	F (%)
Among Columns	Inhibitor concentration	59105.7	5	11821.14	-10.81	2.53	-245.5
Among Rows	Exposure Time	-50377.1	6	-8396.17	7.68	2.42	209.3
Residual	Residual	-32804	30	-1093.47			
Total	Total	-24075.3	41				

5. Conclusion

The corrosion inhibition performance of HPD on mild steel specimens in dilute Sulphuric and hydrochloric acid is slightly dependent on its concentration in the acid solution due to the instantaneous and effective action of the cationic molecules of the HPD compound. HPD showed mixed inhibiting properties as a result of its influence on the Tafel constants of the redox process and the variation of the corrosion potential (*E*cr) values, but with greater affinity for cathodic reactions inhibition, however the total redox process is modified to effectively suppress the corrosion reactions. The inhibition mechanism obeyed the Langmuir isotherm model only forming a monolayer adsorption onto the steel surface through its functional groups, being absorbed through the pi-electrons of the aromatic rings in its molecular structure and as a cationic species. These observations were corroborated with optical microscopy results which showed the remarkable difference in morphology between inhibited and non-inhibited steel specimen. ANOVA

results in the acid solution shows the overwhelming influence of exposure on the inhibition efficiency with a statistical relevance of 253.1% in H_2SO_4 and 209.3% in HCl.

Acknowledgement-The authors are grateful to the Department of Mechanical Engineering, Covenant University for the provision of facilities for the research work

References

[1] F. S. De Souza, A. Spinelli, *Corros. Sci*., **51**(3) (2009) 642-649

[2] A. A Khadom, A. S Yaro, A. S AlTaie, A. A. H. Kadum, *Portug. Electrochim. Acta.*, 27(6) (2009) 699-712

[3] A. Y. Musa, A. A. Khadom, A. A. H. Kadhum, A. Mohamad, M. S. Takriff, *J. Taiwan Inst. Chem. Eng*., **41** (2010) 126-128

[4] A. S. Yaro, N. S. Masih, A. A. Khadom, *Iraqi J. Chem. Petrol. Eng*., **1** (2000) 83-87

[5] S. Junaedi, A. A. Al-Amiery, A. Kadihum, A. A. H. Kadhum, A. Mohamad, *Int. J. Mol. Sci*., **14**(6) (2013) 11915-11928

[6] F. Bentiss, M. Lebrini, M. Lagrenee, *Corros. Sci*., **47** (2005) 2915-9132

[7] U. M. Eduok, S. A. Umoren, A. P. Udoh, *Arabian J. of Chem.*, **5**(3) (2010) 325-337

[8] A. Trowsdale, J. B. Noble, S. J. Harris, I S R Gibbins, G. E. Thompson, G. C. Wood, *Corros. Sci*., **38**(2) (1996) 177-191

[9] R. T. Loto, C. A. Loto, A. P.I. Popoola, T. Fedotova, *Der Pharm. Chem*., **7**(5) (2015) 72-93

[10] O. F. Nwosu, E. Osarolube, L. A. Nnanna, C. S. Akoma, T. Chigbu, *American J. of Mats. Sci*., 4(4) (2014) 178-183

[11] VanderWaals force *available at* http://en.wikipedia.org/wiki/Van_der_Waals_force [Retrieved: 14/01/2016]

[12] R. T. Loto, C. A. Loto, *Int. J. Electrochem. Sci*., **7** (2012) 9423-9440

[13] M. A. Deyab, S. S. Abd El-Rehim, *Int. J. Electrochem. Sci*., **8** (2013) 12613-12627

[14] G. Limousin, J. P. Gaudet, L. Charlet, S. Szenknect, V. Barthes, M. Krimissa, *Appl. Geochem*. **22** (2007) 249-275

[15] S. J. Allen, G. Mckay, J. F. Porter, *J. Colloid Interface Sci*., **280** (2004) 322-333

[16] E. Bulut, M. Ozacar, I. A. Sengil, *Micropor. Mesopor. Mater*. **115** (2008) 234-246

[17] The Langmuir Equation --- an overview of the Langmuir Isotherm. http://www.alfisol.com /IFS/IFS-003/LMMpro-Langmuir.php. [Retrieved: 11/01/2016]

[18] S. Kundu, A. K. Gupta, *Chem. Eng. J*., **122** (2006) 93-106

[19] I. M. Richard, *Principles of Adsorption and Reaction on Solid Surfaces*, 1st ed., Wiley-Interscience, 1996, p. 240.

[20] I. M. Richard, *Principles of Adsorption and Reaction on Solid Surfaces*, Wiley-Interscience. 1996, p. 244.

[21] M. Hosseini, S. F. L. Mertens, M. R. Arshadi, *Corros. Sci*., **45**(7) (2003) 1473-1489

[22] R. F. V. Villamil, P. Corio, J. C. Rubim, S. M. I. Agostinho, *J. Electronalyt. Chem*., **472**(2) (1999) 112-119

[23] K. Vijayaraghavan, T. V. N. Padmesh, K. Palanivelu, M. Velan, *J. Hazard. Mater*., **B133** (2006) 304-308

[24] A. S. Yaro, A. A. Khadom, R. K. Wael, *Alexandria Eng. J*., **52**(1) (2013) 129-135

[25] X. Li, S. Deng, H. Fu, *Corros. Sci*., **53** (2011) 1529-1536